Chinese Chemical Letters 31 (2020) 3135–3138

Contents lists available at ScienceDirect

Chinese Chemical Letters

journal homepage: www.elsevier.com/locate/cclet

Communication

Preparation of hollow mesoporous silica nanorods for encapsulating and slowly releasing eugenol

Tianlu Zhang[a,c,1], Zhiguo Lu[a,c,1], Luyao Zhang[a,c], Yan Li[a,c], Jun Yang[a,c], Jie Shen[a,c], Jianze Wang[a], Yunwei Niu[d,e], Zuobing Xiao[d,e], Lei Chen[b,*], Xin Zhang[a,*]

[a] State Key Laboratory of Biochemical Engineering, Institute of Process Engineering, Chinese Academy of Sciences, Beijing 100190, China
[b] Department of Obstetrics and Gynecology, Navy General Hospital of People Liberation Army, Beijing 100048, China
[c] School of Chemical Engineering, University of Chinese Academy of Sciences, Beijing 100049, China
[d] Shanghai Research Institute of Fragrance and Flavor Industry, Shanghai 200232, China
[e] School of Perfume and Aroma Technology, Shanghai Institute of Technology, Shanghai 200233, China

ARTICLE INFO

Article history:
Received 6 May 2020
Received in revised form 2 July 2020
Accepted 6 July 2020
Available online 7 July 2020

Keywords:
Eugenol
Hollow mesoporous silica nanorods
Mesoporous silica nanorods
Nano-fragrance
Slow release of fragrance

ABSTRACT

Fragrances are widely used in many aspects of our lives. They cannot only make people happy, but also treat many diseases. However, excessively fast evaporation rate is one of the main obstacles to the use of spices. In this study, mesoporous silica nanorods (MSNRs) and hollow mesoporous silica nanorods (HMSNRs) were prepared to encapsulate eugenol. These two nano-fragrances were named eugenol@MSNRs and eugenol@HMSNRs, respectively. The morphologies, size, interior structures and pore performances of MSNRs and HMSNRs. Besides, the performances of encapsulation and fragrance release of eugenol@MSNRs and eugenol@HMSNRs were compared and analyzed. The results showed that eugenol@HMSNRs encapsulated more fragrance and were faster to encapsulate compared with eugenol@MSNRs. Both the release rates of eugenol from eugenol@MSNRs and eugenol@HMSNRs were slow. But the eugenol was released from eugenol@MSNRs more slowly.
© 2020 Chinese Chemical Society and Institute of Materia Medica, Chinese Academy of Medical Sciences. Published by Elsevier B.V. All rights reserved.

With the development of the fine chemical industry, a large number of fragrance molecules can be produced on a large-scale industrialization, which makes fragrances enter many aspects of our lives [1–3]. Many fragrances cannot only improve our quality of life, but also alleviate and treat diseases [4,5]. However, most fragrances are very volatile [6,7]. This results in very strong aromas, which in turn worsen the experience of using the fragrance. Besides, this also leads to a short fragrance retention time, thereby shortening the shelf lives of the fragrance products. Therefore, it is a key challenge for fragrance industry to developing the products that can slowly release fragrances.

Nanotechnology has brought many inspirations to the sustained release of fragrances. Encapsulating fragrances into nanomaterials is an ideal solution to the problem of sustained release of fragrances. There are several types of nanomaterials with sustained release function. Firstly, nanomaterials based on cations can adsorb anionic molecules through electrostatic interaction [8–10]. The degradation or the reversal of charge of cationic nanomaterial causes the disappearance of the electrostatic interaction, thereby releasing anionic molecules. Secondly, the molecules are chemically bonded to the nanomaterial [11–14]. When the chemical bond breaks, the molecule is released. Thirdly, small molecules are encapsulated into nanoparticles such as, micelles and liposomes, to achieve slow release of molecules [15–20]. However, these kinds of nanomaterials are not suitable for loading of most fragrances. In addition, the preparation process of these materials is complicated, and the cost of these materials is high, which leads to a significant increase in the cost of fragrance products and a sharp decline in production. Therefore, this is not an ideal material for slow release of fragrances.

Mesoporous silica nanoparticles (MSNs) have large specific surface areas, so they can adsorb fragrance molecules and slow down the release rate of these molecules [21–25]. MSNs can adsorb most fragrances. In addition, MSNs are now available for mass production at low cost. Therefore, MSNs can be used as an ideal material for sustained release of fragrances. However, traditional MSNs adsorb fragrance molecules through elongated mesoporous channels. This causes two problems: (1) There are less fragrance encapsulated in materials; (2) It takes a longer time to encapsulate fragrances.

* Corresponding authors.
E-mail addresses: chenleis@mail.tsinghua.edu.cn (L. Chen), xzhang@ipe.ac.cn (X. Zhang).
[1] These authors contributed equally to this work.

https://doi.org/10.1016/j.cclet.2020.07.010
1001-8417/© 2020 Chinese Chemical Society and Institute of Materia Medica, Chinese Academy of Medical Sciences. Published by Elsevier B.V. All rights reserved.

In this study, hollow mesoporous silica nanorods (HMSNRs) were designed and prepared to encapsulate eugenol for slow release of fragrance molecules. By contrast, mesoporous silica nanorods were used to encapsulate eugenol. Subsequently, the fragrance encapsulation and release processes of these two silica nanorods loaded with eugenol were compared and analyzed.

Tetraethyl orthosilicate (TEOS, 98%), hexadecyltrimethylammonium bromide (CTAB, 99%), 1-butanol (99.5%), polyvinylpyrrolidone (PVP), average M.W. 8000, K16-K18 and eugenol (98%) were obtained from J&K Scientific. Ammonium hydroxide (28%), ethanol (99%) and sodium carbonate (Na_2CO_3, 99%) were purchased from Sinopharm Chemical Reagent Co., Ltd.

In this study, HMSNRs and mesoporous silica nanorods (MSNRs) were prepared firstly. CTAB (400 mg), ammonium hydroxide (2 mL) and 1-butanol (30 μL) were dissolved into deionized water (95 mL) under ultrasonic condition for 15 min. TEOS (2 mL) was then added into the mixture under stirring at room temperature. After 6 h, the white precipitate (MSNRs-CTAB) was obtained by filtration. The MSNRs-CTAB was then calcined in muffle at 550 °C for 6 h to remove CTAB. The product was MSNRs. The morphology and size of MSNRs were detected by scanning electron microscope (SEM). The internal structure was observed by transmission electron microscope (TEM).

The pore diameter, specific surface area and pore volume of MSNRs were detected by nitrogen adsorption-desorption isotherms and calculated by the Brunauer-Emmett-Teller (BET) method and Barrett-Joyner-Halenda (BJH) method. MSNRs (200 mg) was dissolved into ethanol (80 mL) under ultrasonic condition for 15 min. Deionized water (10 mL), ammonium hydroxide (3 mL) and CTAB (300 mg) were added into this solution under stirring at room temperature for 30 min. TEOS was then added into the mixture under stirring at room temperature. After 6 h, the white precipitate (MSNRs@HMSNRs-CTAB) was obtained by filtration.

The obtained MSNRs@HMSNRs-CTAB was added into deionized water (100 mL). PVP (930 mg) was then added into the mixture under stirring and refluxing. After 3 h, the precipitate (MSNRs@HMSNRs-CTAB-PVP) was obtained by filtration.

The obtained MSNR@HMSNR-CTAB-PVP and Na_2CO_3 (3.18 mg) were then added into deionized water (100 mL) under stirring at room temperature for 30 min. The precipitate (HMSNRs-CTAB-PVP) was then purified by filtration. The morphology and size of MSNRs were detected by SEM. The internal structure was observed by TEM. The pore diameter, specific surface area and pore volume of MSNRs were detected by nitrogen adsorption-desorption isotherms and calculated by the BET method and BJH method. The obtained HMSNRs-CTAB-PVP was then heated in a muffle at 550 °C to remove the PVP and CTAB. The product was HMSNRs.

Then, eugenol@HMSNRs and eugenol@MSNRs were prepared to encapsulate eugenol for slow release of fragrance molecules. HMSNRs (100 mg) and MSNRs (100 mg) were added into eugenol (5 mL) under stirring for 72 h, respectively. The precipitates (eugenol@HMSNRs and eugenol@HMSNRs) were then obtained by filtration and washed three times by ethanol.

The eugenol@HMSNRs (20 mg) and eugenol@HMSNRs (20 mg) were dissolved into ethanol (5 mL), respectively. The two solutions were then taken place into dialysis bag (M.W. 3500) and incubated in ethanol (80 mL) at 25 °C under horizontal shaking (150 rpm). At predetermined time intervals, deionized water (0.5 mL) were removed and the same volume of fresh solution was added. The concentration of vanillin in the deionized water was measured by UV–vis at 278 nm wavelength. The release percentage of drugs was calculated using formula (1):

$$\text{Released percentage (\%)} = W_1/W_2 \times 100\% \quad (1)$$

where W_1 was the weight of eugenol in the PBS, W_2 was the weight of total eugenol in the nanoparticles.

Finally, cytotoxicity assayt was carried out to explore the safety of eugenol@MSNRs and eugenol@HMSNRs. Human skin fibroblast (HSF) cells were purchased from Chinese academy of medical sciences tumor cell bank (Beijing, China). The HSF cells were cultured with DMEM containing 10% fetal bovine serum at 37 °C under 5% CO_2 environment, respectively.

Eugenol@MSNRs and eugenol@HMSNRs with different concentration were added to 100 μL of culture medium, respectively. 20 μL of the MTT solution was added into each well and incubated for additional 2 h after 24 h incubation. The medium and MTT were then replaced with 100 μL of DMSO. The absorbance was measured at 562 nm. Untreated HSF cells were used as control and their cell viability was defined as 100%.

All data were expressed as mean ± SD unless otherwise indicated. Statistical significance was analyzed using one-way ANOVA.

The preparation processes of MSNRs and HMSNRs were shown in Figs. 1A and B. MSNRs were prepared by Stöber method. In brief, ammonium hydroxide catalyzed TEOS to form mesoporous silica nanorods in the case of CTAB as a template agent. The template was removed by calcination. The HMSNRs was prepared based on MSNRs. Firstly, the surface of MSNR was covered with a shell of mesoporous silica shell (MSNR@HMSNR-CTAB). Secondly, the surface of MSNR@HMSNR-CTAB was then covered with a shell of PVP (MSNR@HMSNR-CTAB-PVP). Thirdly, the MSNR core of MSNR@HMSNR-CTAB-PVP was etched by Na_2CO_3. The HMSNR-CTAB shell was not etched by the protection of PVP. Fourthly, the PVP and CTAB were removed by calcination. The product was a HMSNR. In brief, the rod shape of HMSNRs was based on MSNRs. Na_2CO_3 was etching agent and PVP was etching protectant. The organic molecules were finally removed by calcination.

The morphologies of MSNRs and HMSNRs were detected by SEM. As shown in Figs. 2A and B, both the MSNRs and HMSNRs were rod-shaped. The size of HMSNRs was a little bigger than that of MSNRs. The width of MSNRs was about 90 nm and the length of them was about 220 nm. By contrast, the length of HMSNRs was about 260 nm. The internal structure of MSNRs and HMSNRs were observed by TEM. As shown in Figs. 2C and D, the MSNRs was solid. The thin mesoporous channels were observed at the edges of MSNRs. By contrast, HMSNRs were obvious hollow structures.

The mesoporous structures of MSNRs and HMSNRs were detected by nitrogen adsorption-desorption isotherms. As shown in Fig. 3A, the adsorption curve of MSNRs flatten out when $P/P_0 > 0.4$. This result meant that the adsorption reached saturation when $P/P_0 > 0.4$. By contrast, the adsorption curve of HMSNRs steepened when

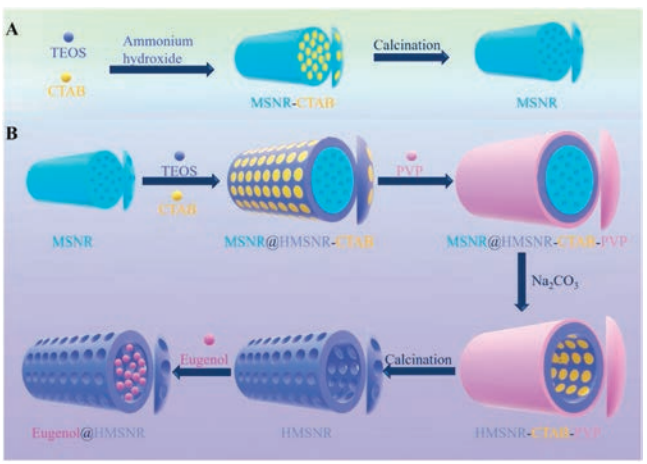

Fig. 1. (A) The schematic diagram of preparation of MSNRs. (B) The schematic diagram of preparation of HMSNRs and eugenol@HMSNRs.

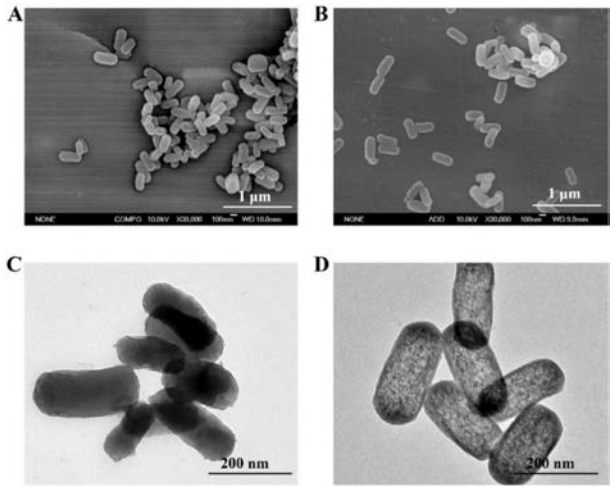

Fig. 2. The SEM images of MSNRs (A) and HMSNRs (B). Scale bar: 1 μm. The TEM images of MSNRs (C) and HMSNRs (D). Scale bar: 200 nm.

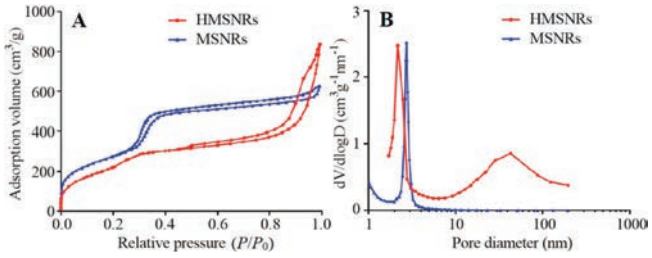

Fig. 3. (A) The nitrogen adsorption-desorption isotherms of MSNRs and HMSNRs. (B) The pore diameter distributions of MSNRs and HMSNRs.

$P/P_0 > 0.8$. This result meant that the nitrogen adsorption capacity rapidly increased, which might be caused by the hollow structures of HMSMRs. The pore sizes of MSNRs and HMSNRs were calculated by a BJH method. As shown in Fig. 3B, the pore diameter of MSNRs was 2.72 nm. The pore diameter of HMSNRs was 6.05 nm. But there were two peaks in the curve of the HMSNRs' pore diameter. One was 2.17 nm and the other was 43.10 nm. The peak of 2.17 nm was the mesoporous structures and the peak of 43.10 nm was the hollow structures. So, the pore diameter of HMSNRs was 2.17 nm. The specific surface areas of MSNRs and HMSNRs were calculate by a BET method and were 1019.64 m^2/g and 850.47 m^2/g, respectively. The specific surface area of MSNRs was larger than the specific surface area of HMSNRs, because MSNRs had more and longer channels. The pore volumes of MSNRs and HMSNRs were calculate by a BJH method and were 1.03 cm^3/g and 1.27 cm^3/g. The pore volume of HMSNRs was bigger than the pore volume of MSNRs.

In the following, eugenol was encapsulated into MSNRs and HMSNRs, respectively. These two kinds of nano-fragrances were named as eugenol@MSNRs and eugenol@HMSNRs. As shown in Fig. 4A, the encapsulation efficiency of eugenol@HMSNRs was 55.9% at 72 h and it was 2.4 times of eugenol@MSNRs. Besides, the encapsulation efficiency of eugenol@HMSNRs was up to 50.4% at 12 h, which was 90.2% of the encapsulation efficiency of eugenol@HMSNRs at 72 h. By contrast, the encapsulation efficiency of eugenol@MSNRs was 15.9% at 12 h, which was 68.3% of the encapsulation efficiency of eugenol@MSNRs at 72 h. Besides, it was not until 36 h that the encapsulation efficiency of eugenol@MSNRs reached more than 90% of the encapsulation efficiency at 72 h. These results proved that HMSNRs could encapsulate fragrance more and faster.

The release profiles of eugenol from eugenol@MSNRs and eugenol@HMSNRs were shown in Fig. 4B. Both eugenol@MSNRs and eugenol@HMSNRs can release fragrances slowly. The release rate of eugenol from eugenol@MSNRs was slightly slower than that of eugenol from eugenol@HMSNRs. This might be caused by two reasons: (1) Eugenol@MSNRs encapsulated less eugenol; (2) The specific surface area of eugenol@MSNRs was larger. Besides, the release rate of eugenol at 37 °C was slight faster than that of eugenol at 25 °C. This might be due to the fact that as the temperature increased, the thermal motion of eugenol was accelerated, which in turn accelerated the diffusion of eugenol.

Most fragrances are used in direct contact with the skin. In order to explore the safety of eugenol@MSNRs and eugenol@HMSNRs, HSF cells were chosen to detect the cytotoxicity of these nanofragrances. As shown in Fig. 4C, the survival rates of HSF cells were still close to 100% when the concentration of eugenol@MSNRs and eugenol@HMSNRs reached 800 μg/mL. Therefore, these two kinds of nano-fragrances have better biosafety.

In summary, mesoporous silica nanorods (MSNRs) and hollow mesoporous silica nanorods (HMSNRs) were prepared to encapsulate eugenol and were named eugenol@MSNRs and eugenol@HMSNRs, respectively. Both MSNRs and HMSNRs were rod-shaped. The HMSNRs were hollow and the size of HMSNRs was a little bigger than the size of MSNRs. The specific surface area of MSNRs was larger and the pore volume of HMSNRs was larger. The eugenol@HMSNRs encapsulated more fragrance and were faster to encapsulate compared with eugenol@MSNRs. Both eugenol@MSNRs and eugenol@HMSNRs could release fragrance slowly. The release rate of eugenol from eugenol@MSNRs was slightly slower than the release rate of eugenol from eugenol@HMSNRs.

Declaration of competing interest

The authors declare that they have no known competing financial interests or personal relationships that could have appeared to influence the work reported in this paper.

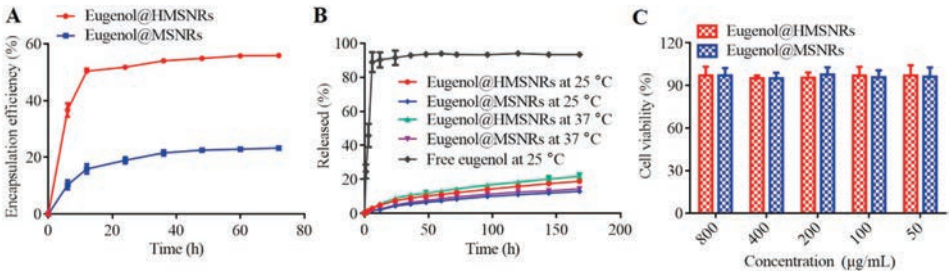

Fig. 4. (A) The encapsulation efficiency of eugenol@MSNRs and eugenol@HMSNRs at different time. (B) The release profiles of eugenol@MSNRs and eugenol@HMSNRs and free eugenol. (C) Effect of eugenol@MSNRs and eugenol@HMSNRs with different concentrations on viability of human HSF cells. The mean ± SD is shown (n = 3).

Acknowledgments

This work was financially supported by the National High Technology Research and Development Program (No. 2016YFA0200303), the Beijing Natural Science Foundation (Nos. L172046, 2192057), the National Natural Science Foundation of China (Nos. 31771095, 21875254 and 21905283).

Appendix A. Supplementary data

Supplementary material related to this article can be found, in the online version, at doi:https://doi.org/10.1016/j.cclet.2020.07.010.

References

[1] S. Burt, Int. J. Food Microbiol. 94 (2004) 223–253.
[2] M.B. Pashazanousi, M. Raeesi, S. Shirali, Asian J. Chem. 24 (2012) 4331–4334.
[3] M.G. Miguel, Flavour. Frag. J. 25 (2010) 291–312.
[4] B. Cooke, E. Ernst, Br. J. Gen. Pract. 50 (2000) 493–496.
[5] B. Ali, N.A. Al-Wabel, S. Shams, et al., Asian Pac. J. Trop. Bio. 5 (2015) 601–611.
[6] A.M. Borda, D.G. Clark, D.J. Huber, B.A. Welt, T.A. Nell, Postharvest. Biol. Tec. 59 (2011) 245–252.
[7] D.L. Berthier, I. Schmidt, W. Fieber, et al., Langmuir 26 (2010) 7953–7961.
[8] Z. Guo, S. Li, Z. Liu, W. Xue, ACS Biomater. Sci. Eng. 4 (2018) 988–996.
[9] J. Zhang, J. Cui, Y. Deng, Z. Jiang, W.M. Saltzman, ACS Biomater. Sci. Eng. 2 (2016) 2080–2089.
[10] Y. Yuan, F. Gong, Y. Cao, et al., J. Biomed. Nanotechnol. 11 (2015) 668–679.
[11] A. Gupta, S. Asthana, R. Konwar, M.K. Chourasia, J. Biomed. Nanotechnol. 9 (2013) 915–925.
[12] L. Song, A. Zeng, M. Hu, et al., J. Biomed. Nanotechnol. 14 (2018) 267–280.
[13] X. Jia, M. Pei, X. Zhao, et al., ACS Biomater. Sci. Eng. 2 (2016) 1641–1648.
[14] D. Li, Y. Song, J. He, M. Zhang, P. Ni, ACS Biomater. Sci. Eng. 5 (2019) 2307–2315.
[15] D.J. Suchyta, M.H. Schoenfisch, ACS Biomater. Sci. Eng. 3 (2017) 2136–2143.
[16] A. Wadi, M. Abdel-Hafez, G.A. Husseini, J. Biomed. Nanotechnol. 15 (2019) 162–169.
[17] D.J. Fu, Y. Jin, M.Q. Xie, et al., Chin. Chem. Lett. 25 (2014) 1435–1440.
[18] Y.H. Niu, T. Yang, R.Y. Ke, C. Wang, Mater. Express 9 (2019) 563–569.
[19] M.C.F. Goncalves, O. Mertins, A.R. Pohlmann, N.P. Silveira, S.S. Guterres, J. Biomed. Nanotechnol. 8 (2012) 240–250.
[20] J.F. Shi, M.G. Sun, X.Y. Li, et al., J. Biomed. Nanotechnol. 11 (2015) 1568–1582.
[21] J. Wang, Z. Teng, Y. Tian, et al., J. Biomed. Nanotechnol. 9 (2013) 1882–1890.
[22] Y.J. Cheng, S.Y. Qin, Y. Ma, et al., ACS Biomater. Sci. Eng. 5 (2019) 1878–1886.
[23] K.M. Rao, S. Parambadath, A. Kumar, C.S. Ha, S.S. Han, ACS Biomater. Sci. Eng. 4 (2018) 175–183.
[24] W.X. Gao, Y.L. Hu, L. Xu, et al., Chin. Chem. Lett. 29 (2018) 1795–1798.
[25] Y. Wang, Y. Yan, J. Cui, et al., Adv. Mater. 22 (2010) 4293–4297.